ELSEVIER

Thermochimica Acta 285 (1996) 25–33

thermochimica acta

Heat capacity and thermodynamic properties of Cr_2As from 5 to 1000 K

Edgar F. Westrum, Jr [a], Jadwiga Sipowska [b], Fredrik Grønvold [c,*], Svein Stølen [c]

[a] *Department of Chemistry, University of Michigan, Ann Arbor, Michigan 48109, USA*
[b] *Department of Chemistry, University of Michigan-Flint, Flint, Michigan 48503, USA*
[c] *Department of Chemistry, University of Oslo, P.O. Box 1033, Blindern, N-0315, Oslo, Norway*

Received 20 November 1995; accepted 3 January 1996

Abstract

The heat capacity of Cr_2As was measured from 5 to 1000 K by adiabatic shield calorimetry. At a temperature of 298.15 K, $C_{p,m}$ is found to be 79.56 J K^{-1} mol^{-1}, $[S_m(T) - S_m(0)]$ is 91.42 J K^{-1} mol^{-1} and $[(H_m(T) - H_m(0)]$ is 14510 J K^{-1} mol^{-1}, where as at 1000 K, $C_{p,m}$ is 103.1 J K^{-1} mol^{-1}, $[S_m(T) - S_m(0)]$ is 201.8 J K^{-1} mol^{-1} and $[(H_m(T) - H_m(0)]$ is 79750 J K^{-1} mol^{-1}.

A λ-type contribution to the heat capacity with maximum at $\sim$ 394 K is due to magnetic disordering of the antiferromagnetic compound. The clearly cooperative part of the transitional entropy is only 1.3 J K^{-1} mol^{-1} over the region 300 to 450 K. The excess heat capacity above that of the lattice plus dilation and conduction electron contributions at temperatures above 150 K indicates that the magnetic excitations persist over a much wider temperature range.

Keywords: Heat capacity; Cr_2As; Magnetic transition; Thermodynamic properties

1. Introduction

Dichromium arsenide belongs to a class of compounds with intriguing magnetic properties for which associated thermal properties are practically unknown. Cr_2As has a tetragonal structure of the Fe_2As type [1–5] and Mn_2As is isostructural. Strictly speaking the structure type refers to the solids only in the high temperature paramagnetic region. The metal atoms are of two types at positions 2a: 000; 1/2, 1/2, 0, and 2c: 0,

* Corresponding author. Fax: 47 22 85 55 65.

PII: S0040-6031(96)02843-2

1/2, z; 1/2, 0, $\bar{z}$ in the space group *P4/nmm*. The positions are completely filled so that successive layers normal to the *c* axis, termed I, II, and II, contain 2*n*, *n*, and *n* chromium atoms. All three compounds are antiferromagnets at ambient temperature with different types of magnetic ordering. For Cr_2As the magnetic unit cell has a doubled *c* axis [6]. The coupling is antiferromagnetic within the I layers and ferromagnetic within II, the succession being, I, II+, II+, I, II−, II−.

Magnetic susceptibility studies have been carried out [2–4,7,8]. They show that the Néel temperature of Cr_2As is ~ 400 K. Neutron spectroscopy studies by Yamaguchi et al. [9] have shown that the magnon dispersion is proportional to the reciprocal lattice vector for small *q*, with slopes of 125 and 185 meV Å along the *c* and *a* axes, respectively. It is suggested that Cr_2As is a system of coexisting itinerant (site I) and localized (site II) 3d-electrons.

The only heat-capcity measurements reported so far are for $Cr_{2.1}As$ by Yuzuri [2] in the form of a graph. It shows a small rounded peak at about 393 K, which indicates that the magnetic excitations extend over a broad range in temperature. The total enthalpy of absorption was estimated to be 200 J per mole of Cr. The heat capacity appears to be about 55 $JK^{-1}mol^{-1}$ at 320 K and 70 JK^{-1} mol^{-1} at 470 K. These values are surprisingly small compared with those for CrAs [10] on a mole of atom basis, 69% at 320 K and 81% at 470 K. Furthermore, the smallness of the clearly cooperative part of the magnetic transition in Cr_2As has its counterpart in those of chromium with heat capacity ($C_{p,m}$ = 32.7 JK^{-1} mol^{-1} at 1000 K) [11], or 30% above the classical limit, as well as that of CrAs($C_{p,m}$ = 67.3 JK^{-1} mol^{-1} at 1000 K) [10]. More accurate delination is also needed for Cr_2As.

A further interest in the thermodynamic properties of Cr_2As stems from the use of chromium as contact material in semiconductor devices. Phase analytical studies and phase diagram calculations for ternary M–Ga–As systems have been performed [12–14].

The ternary Cr–Ga–As system is important for two reasons. In addition to the use of chromium films in semi-metal contacts, a large number of GaAs devices are made using Cr-doped GaAs substrates [15]. In either case interfacial reactions are reported. Cr_2As and/or $GaCr_2$ are presumably formed when a chromium film on GaAs is heated to temperatures above 673 K [16,17]. Furthermore, the use of Cr-doped GaAs is problematic due to the redistribution of chromium with the formation of new compounds as inclusions. Also for this reason the thermodynamic properties of Cr_2As are considered to be of interest.

2. Experimental

Cr_2As was prepared from high-purity chromium and arsenic. The electrolytic hydrogen-treated Cr flakes were a gift from Dr. Warren DeSorbo and the Research Laboratory of General Electric at Schenectady, U.S. It contained less than 70 ppm Fe, less than 100 ppm total of other metals, and less than 60 ppm of oxygen. The As was 99.9999 metallic lumps from Koch-Light Laboratories Ltd. The mixture of the elements was heated in evacuated, sealed fused silica tubes. The temperature in the

horizontally positioned furnace was increased in steps of 30 K each 8 h to 1170 K. After cooling the sample to room temperature for 1 d it was crushed and subjected to a further annealing at 970 K for 14 d.

Room temperature X-ray powder photographs were taken by the Guinier technique using $CuK\alpha_1$ radiation and silicon as an internal standard [18]. Unit-cell dimensions were derived by least squares refinement. The presently derived unit-cell dimensions and earlier values are given in Table 1. Our values agree well with those by Fruchart [20]. Deviations by other authors with regard to the length of the *a* axis point to compositional differences.

The low temperature heat capacity measurements at Ann Arbor were performed in the Mark XIII adiabatic cryostat [21]. About 166 g of sample was loaded into the calorimeter of mass 29.46 g and internal volume of 44.7 cm^3. In order to facilitate rapid thermal equilibration, a pressure 3.6 kPa at 300 K of He gas was introduced after prior evacuation of the calorimeter. The thermometer was calibrated by the US National Bureau of Standards against IPTS-68, and was considered to reproduce thermodynamic temperatures within 0.03 K between 5 K and 300 K. The heat capacity of the empty calorimeter represented about 25% of the total heat capacity below 50 K, decreasing to about 18% at ambient temperature. Below 10 K the standard deviation of a single measurement is about 4%, up to 250 K about 0.09% and above this range about 0.2%.

The high-temperature calorimetric apparatus and measuring technique have been described earlier [22, 23] along with results obtained for the heat capacity of a standard sample of α-Al_2O_3. The calorimeter is intermittently heated, and surrounded by electrically heated, and electronically controlled adiabatic silver shields. A heated guard system, also of silver, is outside the shields and the whole assembly is placed in a vertical tube furnace. The temperature differences between corresponding parts of the calorimeter and shield are measured by means of Pt–(Pt + 10 mass% Rh) thermopiles. The amplified signals are recorded and also used for automatic control of the shield heaters to maintain quasi-adiabatic conditions during input and drift periods. The temperature of the guard body is kept 0.4 K below that of the shield, while the

Table 1
Unit cell dimensions of Cr_2As at ambient temperature

a/pm	*c*/pm	Ref.
362.0[a]	634.6[a]	[1]
358	625	[2]
359.5	634.4	[4]
360	634	[6]
361.8	635.0	[19]
359.4	634.6	[20]
359.2 ± 0.5	635.1 ± 0.5	This work

[a] Transformed from kX to pm by multiplication by 100.02.

temperature of the furnace is kept 10 K lower to ensure satisfactory operation of the control units.

The mass of the sample used in the experiments was about 170 g. It was enclosed in an evacuated and sealed vitreous silica tube of about 50 cm^3 volume, which fit tightly into the silver calorimeter. A central well in the tube serves for the heater and the platinum resistance thermometer which was calibrated locally, at the ice, steam, tin, zinc, and antimony points. Temperatures are judged to correspond with ITS-90 to within 0.05 K from 300 to 900 K, and within 0.1 K at 1000 K. The energy inputs from a constant-current supply are measured with a Hewlett–Packard digital voltmeter with an accuracy of 0.025%.

The heat capacity of the calorimeter without a sample was determined in a separate series of experiments with a standard deviation of a single measurement from the smoothed heat capacity curve of about 0.15%. The heat capacity of the empty calorimeter represented approximately 60% of the total heat capacity. Small corrections were applied for differences in mass of the empty and full vitreous silica containers and for the "zero" drift of the calorimeter. The standard deviation for a single measurement up to 394 K is 0.35%. In the higher temperature region it is 0.49%. The accuracy in the derived thermodynamic functions is estimated to be 0.15% at 300 K and decreases to 0.35% at 1000 K.

3. Results and discussion

The experimental heat capacities are given in chronological order in Table 2 and are presented graphically in Fig. 1. The approximate temperature increments used in the determinations can usually be inferred from adjacent mean temperatures in Table 2. A λ-type heat-capacity maximum connected with the antiferro- to para-magnetic transition is observed at $\sim$ 394 K, in good agreement with the earlier determination of the Néel temperature by Yuzuri [2]. Others diverge more: 408 K [8]; 440 K [4]. The transition was mapped with two series of determinations. The maximum mean heat capacity is 99.0 $J\,K^{-1}\,mol^{-1}$ over a 0.607 K interval around 394.39 K.

The experimental heat capacities were fitted to polynomials in temperature by the method of least squares. Values of enthalpy and entropy were obtained by integration of the heat-capacity polynomials. Extrapolation to $T = 0$ K was made by fitting the heat-capacity values below 17 K to the equation $C_{p,m} = \gamma t + \alpha T^3$. An approximate value for the conduction electron heat capacity coefficient $\gamma = 4.5$ mJ $K^{-2}\cdot mol^{-1}$ was obtained. Function values at selected temperatures are given in Table 3.

Estimates of the more cooperative part of the transitional enthalpy and entropy may be obtained by bridging the heat capacity across the 300 to 470 region with the polynomial $C_{p,m} = 9.6 + 0.42(T/K) - 7.735\cdot10^{-4}(T/K)^2 + 4.95\cdot10^{-7}(T/K)^3$, see Fig. 1. In this way we obtain $\Delta_{trs}H_m = 490\,J\,mol^{-1}$ and $\Delta_{trs}S_m = 1.31\ J\ K^{-1}\ mol^{-1}$. A comparison with the value given by Yuzuri [2], 200 $J\,mol^{-1}$ is hampered by uncertainty about which entity he refers to. According to the text it appears to be Cr, but from Fig. 9 in his paper the excess enthalpy over the region 370 to 420 K appears to be $\sim$ 70 $J\,mol^{-1}$ for Cr, or $\sim$ 200 $J\,mol^{-1}$ for $Cr_{2.1}As$. The actual heat-capacity results

Table 2
Molar heat capacity of Cr_2As {M(Cr_2As) = 178.9138 g mol^{-1}}

T/K	$C_{p,m}$/J K^{-1} mol^{-1}	T/K	$C_{p,m}$/J K^{-1} mol^{-1}	T/K	$C_{p,m}$/J K^{-1} mol^{-1}
University of Oslo					
Series I		340.28	85.42	Series III	
306.32	80.41	349.75	86.83	717.67	94.30
315.95	81.98	355.20	86.86	737.17	94.62
325.50	83.07	356.67	87.74	743.67	95.01
335.03	84.63	358.15	87.64	750.17	95.34
344.51	85.83	359.64	87.87	756.67	95.63
353.90	87.38	361.13	88.11		
363.23	88.99	362.62	88.43	Series IV	
372.46	91.04	364.10	88.82	797.25	95.88
381.65	92.94	365.58	88.82	802.16	95.60
390.70	96.79	367.05	89.48	807.87	96.50
399.87	90.79	368.53	90.06	816.60	97.07
409.32	88.08	370.01	90.21	827.58	97.33
418.96	87.36	371.47	91.28	838.51	97.94
428.62	86.97	373.71	91.24	849.46	98.26
438.36	87.13	376.72	91.46	860.40	98.62
448.09	87.05	379.62	92.35	876.37	99.55
457.89	87.31	382.62	93.00	887.35	100.12
467.71	87.27	385.60	93.91	898.37	100.30
477.59	87.35	387.79	94.84	909.40	100.68
487.25	87.44	388.78	94.92	920.43	101.19
497.22	87.67	389.34	95.20	931.56	101.14
507.23	87.68	389.91	95.58	942.71	101.14
517.29	88.03	390.47	95.93	953.97	101.22
527.42	87.68	391.04	96.67	965.24	103.05
537.57	88.46	391.60	96.86	976.45	102.50
547.71	89.10	392.16	97.20	987.85	102.39
557.84	88.54	392.72	97.34	999.37	103.25
567.94	89.55	393.28	98.37		
588.33	90.52	393.84	98.45	Series V	
598.74	90.20	394.39	99.02	674.73	92.99
609.11	90.90	394.95	97.74	685.21	93.34
619.53	90.95	395.52	93.80	695.73	93.62
629.96	91.99	396.09	92.31	706.25	93.75
640.42	91.68	396.67	91.63	716.81	94.15
650.92	91.99	397.25	91.15	727.40	94.42
661.46	92.47	399.10	90.23	738.02	95.00
672.03	92.45	402.08	88.68	748.68	95.48
		405.16	88.60	759.68	95.69
Series II		408.28	87.58	770.13	96.20
301.67	80.13	411.35	87.95	823.06	97.34
311.50	81.34	414.50	87.04	833.99	97.82
321.17	82.70	417.62	87.71	844.89	98.65
330.73	84.00	420.80	86.89	855.74	99.35
University of Michigan					
Series VI		36.536	6.544	246.119	73.18
5.08	0.047	38.668	7.541	253.319	73.99

Table 2 (*Continued*)

T/K	$C_{p,m}$/J K^{-1} mol^{-1}	T/K	$C_{p,m}$/J K^{-1} mol^{-1}	T/K	$C_{p,m}$/J K^{-1} mol^{-1}
6.421	0.076	41.017	8.730	264.133	75.39
7.350	0.082	43.381	9.928	274.942	76.74
8.255	0.108	45.770	11.233	282.157	77.60
9.363	0.166	48.444	12.713	289.502	78.57
10.493	0.241	51.392	14.426	296.947	79.39
11.449	0.224	54.355	16.16	304.362	80.28
12.477	0.349	57.355	17.89	311.765	80.93
13.565	0.424	60.646	19.90	319.185	81.83
15.447	0.632	64.237	21.79	326.594	82.63
17.493	0.820	67.819	24.15	334.009	83.31
		71.459	26.22	342.482	84.10
Series VII		75.398	28.53		
6.723	0.067	79.640	30.82	Series VIII	
7.471	0.096	86.059	34.33	94.169	38.45
9.098	0.180	95.606	39.05	99.078	40.58
10.515	0.224	102.498	42.12	103.825	42.75
11.598	0.268	107.271	44.11	110.999	45.78
12.820	0.391	112.064	46.00	118.197	48.60
14.095	0.474	117.185	48.15	123.011	50.49
15.430	0.599	122.669	50.43	127.848	52.19
16.809	0.748	115.430	47.50	132.700	53.86
17.492	0.820	120.324	49.51	137.702	55.56
18.212	0.948	125.345	51.29	142.865	57.01
19.637	1.156	130.385	53.11	148.042	58.49
21.070	1.422	135.429	54.82	153.235	59.66
22.596	1.738	176.278	63.62	158.438	60.69
24.216	2.112	181.837	64.43	163.650	61.79
25.849	2.536	191.081	65.69	168.997	62.49
27.501	3.026	203.426	67.46	174.455	63.30
29.151	3.575	215.785	69.15	182.623	64.46
30.909	4.182	225.024	70.32	190.796	65.76
32.767	4.922	231.711	71.21	196.247	66.47
34.639	5.729	238.927	72.19	204.408	67.63

of Yuzuri [2], obtained in an adiabatic calorimeter, are only about 3/4 of those obtained here in the region 320 to 470 K. They are superseded by the present results.

The transitional entropy contribution considered so far, 1.31 J K^{-1}·mol^{-1} over the region 300 to 450 K is only a fraction of that expected for randomization of 3d electron spins on chromium. According to Goodenough [24] Cr_2As has the charge configuration $Cr^+Cr^{2+}As^{3-}$. The corresponding spin-only entropy contribution from $3d^5$ and $3d^4$ electron randomization is $R\ln 6 + R\ln 5 = 28.28$ J K^{-1} mol^{-1} for the high-spin alternative and $R\ln 2 + R\ln 3 = 14.90$ J K^{-1} mol^{-1} for the low-spin alternative.

In the structure of Cr_2As each Cr(I) atom in addition to being bonded tetrahedrally to 2As at $d = 250$ pm and 2As at 255 pm, is also bonded to 4Cr(I) in planar quadratic

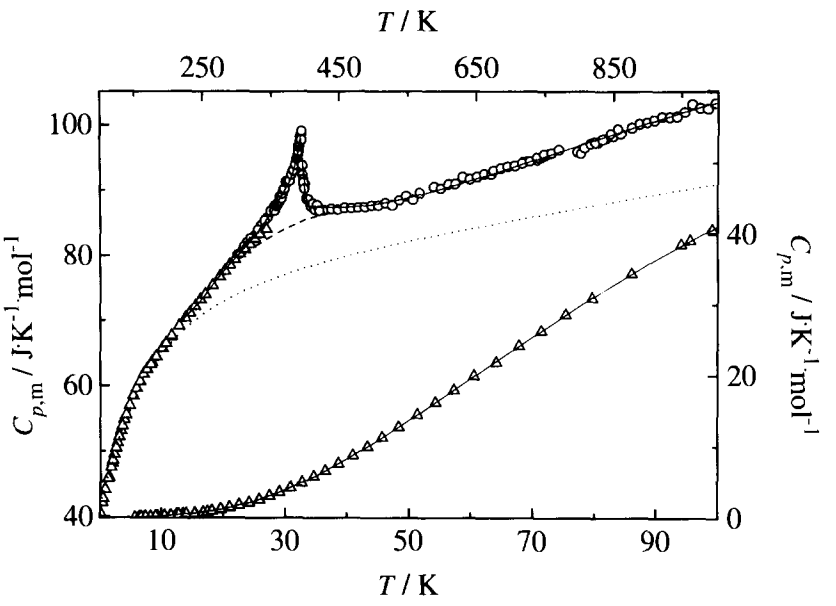

Fig. 1. Molar heat capacity of Cr_2As. Δ, present results University of Michigan ○, present results University of Oslo; ···, C_p(lattice) = C_V(lattice) + C_{el} + C_{dil}; – – –, estimated C_p background for clearly cooperative part of transition.

fashion at $d = 255$ pm. The calculated distances are based upon the z-parameter values reported by Watanabe et al. [5]. The Cr(I)–Cr(I) distances are not much larger than in bcc chromium metal, d(Cr–8Cr) = 250 pm, and may account for the antiferromagnetic coupling and low magnetic moment of Cr(I) in Cr_2As. The Cr(II) atoms are bonded to five As atoms at the corners of a square pyramid, d(Cr(II)–4As) = 257 pm, d(Cr(II)–1 As) = 254 pm. The nearest chromium neighbours, Cr(II)–2Cr(I), are 273 pm away. The longer distance implies reduced interaction, which may partly be responsible for the higher magnetic moment of Cr(II) observed in the neutron diffraction study of Cr_2As by Yamaguchi et al. [6]. The chromium atoms at sites I and II were found to have magnetic moments of 0.40 μ_B and 1.36 μ_B at 130 K. Assuming that 0.40 spins per Cr(I) and 1.34 spins per Cr(II) atoms become completely randomized above T_N the spin-only magnetic entropy should be $\Delta_{mag}S_m = R\ln(2S + 1) = 9\,J\,K^{-1}\,mol^{-1}$. Even this value is far above that observed and indicates that magnetic excitations of a less cooperative nature are of importance. Indications to the same effect arise from the high-temperature susceptibility results for Cr_2As [2,5] which give a mean effective magnetic moment of about 1.5 μ_B per chromium atom at 800 K. Hollan [4] reports a slightly lower effective moment in this temperature region and $(3.5 \pm 1)\,\mu_B$ as the high-temperature limit.

In order to get an estimate of the over-all magnetic heat capacity, the contributions due to harmonic and anharmonic lattice vibrations and conduction electrons must be subtracted from the total. In the temperature range up to ~ 200 K one can estimate the lattice heat capacity at constant volume from the experimental values, $C_{p,m}$ by

Table 3
Thermodynamic properties at selected temperatures for Cr_2As {$M(Cr_2As) = 178.9138\,g\,mol^{-1}$}

T/K	$C_{p,m}$/(J K^{-1} mol^{-1})	$H_m(T) - H_m(0)$/(J mol^{-1})	$S_m(T) - S_m(0)$/(J K^{-1} mol^{-1})	$-[G_m(T) - H_m(0)]$/(J K^{-1} mol^{-1})
5	(0.033)	(0.081)	(0.029)	(0.013)
10	0.208	0.628	0.099	0.036
15	0.582	2.543	0.248	0.078
20	1.222	6.883	0.498	0.154
25	2.303	15.48	0.872	0.253
30	3.875	30.75	1.429	0.404
35	5.853	54.90	2.169	0.600
40	8.215	89.94	3.100	0.852
45	10.817	137.4	4.215	1.162
50	13.627	198.5	5.495	1.525
60	19.48	363.8	8.496	2.433
70	25.39	588.3	11.947	3.543
80	31.10	871.0	15.71	4.826
90	36.35	1209	19.68	6.250
100	41.04	1596	23.76	7.802
120	49.34	2501	31.99	11.140
140	56.30	3561	40.14	14.703
160	61.00	4738	47.99	18.39
180	64.24	5992	55.37	22.09
200	67.00	7304	62.28	25.76
220	69.70	8671	68.79	29.38
240	72.38	10092	74.98	32.93
260	74.88	11565	80.87	36.39
280	77.43	13088	86.52	39.78
298.15	79.56	14513	91.45	42.77
300	79.77	14660	91.94	43.07
350	86.69	18812	104.7	50.97
394.4	99.0	(22800)	(115.5)	(57.56)
400	88.47	23370	116.89	58.46
450	87.38	27750	127.21	65.53
500	87.84	32130	136.43	72.17
550	88.86	36550	144.85	78.40
600	90.22	41020	152.64	84.27
650	91.80	45570	159.92	89.81
700	93.48	50200	166.79	95.07
750	95.21	54920	173.29	100.06
800	96.93	59730	179.49	104.83
850	98.61	64610	185.42	109.41
900	100.2	69590	191.1	113.8
950	101.7	74630	196.6	118.0
1000	103.1	79750	201.8	122.1

subtracting the dilation and conduction electron contributions. The anharmonic dilation contribution is estimated using values for the thermal expansivity, $\alpha = 8.2 \times 10^{-5}\ K^{-1}$ (293 to 483 K) [5] and the Grüneisen parameter $\Gamma = 2$, from values for similar substances. The dotted non-transitional heat capacity curve shown in Fig. 1 corresponds to a Debye-type heat capacity, $\Theta_D = 375$ K, plus conduction electron and dilation contributions. The Debye temperature was chosen as the maximum in a plot of the Debye temperature calculated from each individual heat-capacity determination versus temperature. The maximum was obtained at $\sim$ 100 K after which the apparent Debye temperature decreases abruptly due to contributions from the magnetic order–disorder transition. The resulting magnetic enthalpy and entropy increments over the temperature range 150 K to 1000 K are $\Delta_{trs}H_m = 6720$ J mol^{-1} and $\Delta_{trs}S_m = 12.3$ J K^{-1}. The latter value is intermediate between the magnetic entropy increment expected from the neutron diffraction results [6] and that from low spin $3d^5$ and $3d^4$ electron randomization.

References

[1] H. Nowotny and O. Årstad, Z. Phys. Chem. Abt. B: 38 (1938) 461.
[2] M. Yuzuri, J. Phys. Soc. Jpn., 15 (1960) 2007.
[3] L. Hollan, P. Lecocq and A. Michel, Compt. rend. Paris, 260 (1965) 2233.
[4] L. Hollan, Ann. Chim. France, 1 (1966) 437.
[5] H. Watanabe, Y. Nakagawa and K. Sato, J. Phys. Soc. Jpn., 20 (1965) 2244.
[6] Y. Yamaguchi, H. Watanabe, H. Yamaguchi and S. Tomiyoshi, J. Phys. Soc. Jpn., 32 (1972) 958.
[7] H. Haraldsen and E. Nygaard, Z. Elektrochem., 45 (1939) 686.
[8] A. Krumbügel Nylund, D. Boursier, A. Rouault, J. P. Senateur and R. Fruchart, Mater. Res. Bull., 9 (1974) 21.
[9] Y. Yamaguchi, A.I. Goldman, K. Ishimoto and M. Ohashi, J. Magn. Mater., 70 (1987) 197.
[10] R. Blachnik, G. Kudermann, F. Grønvold, A. Alles, B. Falk and E.F. Westrum, Jr. J. Chem. Thermodyn., 10 (1978) 507.
[11] R. Hultgren, P.D. Desai, D.T. Hawkins, M. Gleiser, K.K. Kelley and D.D. Wagman, Selected Values of the Thermodynamic Properties of the Elements, Am. Soc. Metals, OH, 1973.
[12] T. Sands, J. Metals, 38 (1986) 31.
[13] R. Schmid-Fetzer, J. Electron. Mater., 17 (1988) 193.
[14] J.C. Lin and Y.A. Chang, High Temp. Sci., 26 (1990) 365.
[15] M.D. Deal, R.A. Gasser and D.A. Stevenson, J. Phys. Chem. Solids, 46 (1985) 859.
[16] S.D. Mukherjee, D.V. Morgan, M.J. Smith and P. Brook, J. Vac. Sci. Technol., 16 (1979) 138.
[17] S.D. Mukherjee, C.J. Palmstrøm and J.G. Smith, J. Vac. Sci. Technol., 17 (1980) 904.
[18] R.D. Deslattes and A. Henins, Phys. Rev. Lett., 31 (1973) 972.
[19] A. Kjekshus and K.E. Skaug, Acta Chem. Scand., 26 (1972) 2554.
[20] R. Fruchart, Ann. Chim. France, 7 (1982) 563.
[21] E.F. Westrum, Jr., G.T. Furukawa and J.P. McCullough, Experimental Thermodynamics, Vol. I. J.P. McCullough and D.W. Scott (Eds.), Butterworths, London, 1968, p. 113.
[22] F. Grønvold, Acta Chem. Scand, 21 (1967) 1695.
[23] F. Grønvold, J. Chem. Thermodyn., 25 (1993) 1133.
[24] J.B. Goodenough, Magnetism and the Chemical Bond, Interscience-Wiley, New York, London, 1963, p. 295.